manuscript No.
(will be inserted by the editor)

Resonant Tunneling of Wannier-Stark-States

Markus Glück, Andrey R. Kolovsky and H. Jürgen Korsch

Fachbereich Physik, Universität Kaiserslautern, D-67653 Germany.

November 26, 1999

Abstract. An effective method of calculating Stark resonances is deduced from a scattering theory for Stark systems. The method is applied to the problem of a Bloch-particle in a constant external field. When the field strength is varied over a wide range, resonant tunneling can be observed. The resonance widths as a function of the field strength can be accurately described by a few-state model.

PACS. 0 3.80.+r, 73.20.Dx, 73.40.Gk

1 Introduction

We study the lifetime of Wannier-Stark-states, i.e. of metastable eigenstates of the Hamiltonian

$$H = \frac{p^2}{2} + V(x) + Fx, \quad V(x+2\pi) = V(x)\,. \qquad (1)$$

These eigenstates are arranged in families of resonances with equidistant spacing, the so-called Wannier-Stark-ladders of resonances. While for a long time this field was mainly of theoretical interest (and gave rise to some controversies, see, e.g., [1–3]), the recent experiments with cold neutral atoms in a standing laser wave [4–6] allow an almost perfect experimental realization of the Hamiltonian (1). Theoretical predictions as Wannier-Stark-ladders [4] and Bloch oscillations [5] have been verified and, for the first time, the tunneling rate has been directly measured [7].

The present paper theoretically analyzes the dependence of the tunneling rate on the system parameters. It is organized as follows. In Sec. 2 we introduce the scattering matrix (S-matrix) for Stark systems. Then, analyzing its structure, a simple and direct method of calculating its poles (i.e. the resonances) is developed. The tunneling rate of the system is then found as the imaginary part of the resonance energy $\mathcal{E}$.

In Sec. 3, we explain the effects of resonant tunneling heuristically. Using scaled variables, the Hamiltonian (1) has two parameters, the field strength F and the scaled Planck constant $\hbar$. While the field strength directly influences the lifetime, a variation of $\hbar$ changes the number of bound states in the potential $V(x)$ and, therefore, the number of long-lived resonances. The most simple situation is given for large $\hbar$, which is investigated in Sec. 4. A two state model description is introduced, which yields an analytical expression for the lifetime as a function of the field strength F. In Sec. 5, the case of smaller $\hbar$, where more bound states exist, is analyzed. The model description of Sec. 4 is adjusted and shown to yield accurate results even in this parameter range.

2 Scattering Theory for Stark-Systems

The Stark Hamiltonian is given by

$$H = \frac{p^2}{2} + Fx + V(x)\,, \qquad (2)$$

where the potential $V(x)$ is bounded, i.e. $|V(x)| < const$, and $F > 0$. Asymptotically, the field term Fx dominates the potential $V(x)$, therefore it is convenient to treat $V(x)$ as a perturbation of $H_0 = p^2/2 + Fx$. The combined potential $V(x) + Fx$ cannot support bound states, because any state can decay in the negative x-direction. The states are metastable, i.e. they are resonance states, and scattering theory can be used to calculate the resonances of the Stark system, i.e. the poles of the S-Matrix $\mathbf{S}(E)$.

In the next section we give a definition of the matrix $\mathbf{S}(E)$. We note that this definition is valid for arbitrary bounded potentials $V(x)$. Later on, however, we restrict ourselves to periodic potentials, which is the case of our primary interest.

2.1 S-Matrix for Stark-Systems

The matrix elements of the S-Matrix $\mathbf{S}(E)$ are calculated by comparison of the asymptotes of the scattering states $\Psi_S(E)$ with the asymptotes of the "unscattered" states $\Psi_0(E)$, which are the eigenstates of the "free" Hamiltonian

$$H_0 = \frac{p^2}{2} + Fx\,, \quad F > 0. \qquad (3)$$

In configuration space the $\Psi_0(E)$ are Airy functions

$$\langle x|\Psi_0(E)\rangle \sim \mathrm{Ai}\,(\xi - \xi_0) \tag{4}$$

with $\xi = ax$, $\xi_0 = aE/F$ and $a = (2F/\hbar^2)^{1/3}$. For $\xi \to -\infty$, the Airy functions tend to

$$\mathrm{Ai}(\xi) \sim \xi^{-1/4} \sin\left(\zeta + \pi/4\right) \tag{5}$$

with $\zeta = 2/3\,\xi^{3/2}$. Actually, in the Stark case it is more convenient to compare the momentum space asymptotes instead of the configuration space asymptotes. Indeed, both approaches are equivalent, which will be shown below. In momentum space the eigenstates $\Psi_0(E)$ are given by

$$\langle k|\Psi_0(E)\rangle = \exp\left[\mathrm{i}\left(\frac{\hbar^2 k^3}{6F} - \frac{Ek}{F}\right)\right]. \tag{6}$$

For $F > 0$ the direction of decay is the negative x-axis, so the limit $k \to -\infty$ of $\langle k|\Psi_0(E)\rangle$ is the outgoing part and the limit $k \to \infty$ the incoming part of the free solution.

The scattering states $|\Psi_S(E)\rangle$ solve the Schrödinger equation

$$H|\Psi_S(E)\rangle = E|\Psi_S(E)\rangle \tag{7}$$

with $H = H_0 + V(x)$. Asymptotically the potential $V(x)$ can be neglected and the scattering states are eigenstates of the free Hamiltonian (7). In other words, we may say, that

$$\lim_{k\to\pm\infty} \langle k|\Psi_S(E)\rangle = \exp\left[\mathrm{i}\left(\frac{\hbar^2 k^3}{6F} - \frac{Ek}{F} + \varphi_\pm(E)\right)\right]. \tag{8}$$

In terms of the phase shifts $\varphi_\pm$ the S-matrix reads $\mathbf{S}(E) = \exp(\mathrm{i}\varphi_-)/\exp(\mathrm{i}\varphi_+)$, which with the help of Eq. (8) yields the definition

$$\mathbf{S}(E) = \lim_{k\to\infty} \frac{\langle -k|\Psi_S\rangle}{\langle -k|\Psi_0\rangle}\frac{\langle k|\Psi_0\rangle}{\langle k|\Psi_S\rangle}, \tag{9}$$

which we will use in the following. Now we show that defining the S-matrix via the momentum space asymptotes is equivalent to the usual approach via the configuration space asymptotes. Indeed, let us write $\langle k|\Psi_S(E)\rangle$ as

$$\langle k|\Psi_S(E)\rangle = \exp\left[\mathrm{i}\left(\frac{\hbar^2 k^3}{6F} - \frac{Ek}{F} + \varphi(k)\right)\right], \tag{10}$$

where $\varphi(\pm k) \to \varphi_\pm$ for $k \to \pm\infty$, i.e. $\varphi(\pm k) \approx const$ asymptotically. Fourier transform of Eq. (10) yields

$$\langle x|\Psi_S(E)\rangle \sim \int_{-\infty}^{\infty} \mathrm{d}k \exp\left[\mathrm{i}\left(k(x - \frac{E}{F}) + \frac{\hbar^2 k^3}{6F} + \varphi(k)\right)\right], \tag{11}$$

where the free solution is included by $\varphi(k) = 0$. The asymptotes of $\langle x|\Psi_S(E)\rangle$ for $x \to -\infty$ can be found, e. g., by the method of steepest descent. Losely speaking, this means, that in the limit $x \to -\infty$ only the stationary points of the phase

$$\theta(k) = k(x - E/F) + \hbar^2 k^3/6F + \varphi(k) \tag{12}$$

contribute to the integral Eq. (11). If we assume that $\varphi(k)$ is approximately constant for large $|k|$, the solutions of $\theta'(k) = 0$ are

$$k_\pm = \pm\sqrt{2(E - Fx)}\,/\hbar. \tag{13}$$

Indeed, the assumption is justified, because $x \to -\infty$ implies $k_\pm \to \pm\infty$, which is the region where the assumption holds. Therefore, in the free and in the scattered case, the *same* stationary points $k_\pm$ contribute to the integral (11).

The separation between incoming and outgoing wave is trivial: k_+ contributes to the incoming and k_- to the outgoing part of the wavefunctions. Then, the asymptotically outgoing part of $\langle x|\Psi_S(E)\rangle$ is

$$\lim_{x\to-\infty} \langle x|\Psi_{S,\mathrm{out}}\rangle \sim \theta''(k_-)^{-1/2} \exp\left(\mathrm{i}\,\theta(k_-)\right). \tag{14}$$

with $\theta''(k) = \hbar^2 k/F$. Analogously, the incoming part is given by inserting k_+. With the help of $\langle k|\Psi_S\rangle = \exp(\mathrm{i}\theta(k))$ and the cancellation of the prefactors $\theta''(k)^{-1/2}$ of the free and the scattered solution, we get

$$\lim_{x\to-\infty} \frac{\langle x|\Psi_{S,\mathrm{out}}\rangle}{\langle x|\Psi_{0,\mathrm{out}}\rangle}\frac{\langle x|\Psi_{0,\mathrm{in}}\rangle}{\langle x|\Psi_{S,\mathrm{in}}\rangle} = \lim_{k\to\infty} \frac{\langle -k|\Psi_S\rangle}{\langle -k|\Psi_0\rangle}\frac{\langle k|\Psi_0\rangle}{\langle k|\Psi_S\rangle}. \tag{15}$$

Therefore, using the momentum space asymptotes for the calculation of the S-Matrix is equivalent to using the configuration space asymptotes.

2.2 The Floquet-Bloch-solutions

From here on we consider the case of a 2π-periodic potential $V(x + 2\pi) = V(x)$. Then, we introduce the states $|\Phi_S(E)\rangle$, which instead of Eq. (7) solve the time-dependent equation

$$\exp\left(-\mathrm{i}\frac{H\tau_\mathrm{B}}{\hbar}\right)|\Phi_S(E)\rangle = \exp\left(-\mathrm{i}\frac{E\tau_\mathrm{B}}{\hbar}\right)|\Phi_S(E)\rangle, \tag{16}$$

where τ_B is the so-called Bloch-time $\tau_\mathrm{B} = F/\hbar$. In this case, the time evolution operator $U(\tau_\mathrm{B}) = \exp\left(-\mathrm{i}H\tau_\mathrm{B}/\hbar\right)$ commutes with the translation $x \to x + 2\pi$ [8]. This enables us to make use of a Bloch ansatz, which takes into account the periodicity of the system, which, although violated in the Hamiltonian, still shows up in the classical equations of motion and which quantum mechanically implies the existence of the Wannier-Stark-ladder. It is straightforward to show that there is a one to one relation between solutions of Eq. (7) and of Eq. (16). Clearly, any solution of Eq. (7) solves Eq. (16). On the other hand, suppose $|\Phi_S(E,t)\rangle$ is a quasienergy solution of Eq. (16), i.e.

$$U(t)\,|\Phi_S(E,0)\rangle = \exp\left(-\mathrm{i}\frac{Et}{\hbar}\right)|\Phi_S(E,t)\rangle, \tag{17}$$
$$|\Phi_S(E,t+\tau_\mathrm{B})\rangle = |\Phi_S(E,t)\rangle,$$

where E is any energy of the Floquet ladder $E_l = E_0 + 2\pi l\hbar/\tau_B$. Let us define a new function

$$|\Psi_S(E,t)\rangle = \int_0^{\tau_B} \mathrm{d}t' \exp\left(\frac{\mathrm{i}Et'}{\hbar}\right) U(t'+t)|\Phi_S(E,0)\rangle\,. \tag{18}$$

Because of $\mathrm{i}\hbar\partial_t U(t) = HU(t)$, $|\Psi_S(E,t)\rangle$ solves the time-dependent Schrödinger equation. Furthermore, because of Eq. (17), we get

$$|\Psi_S(E,t)\rangle = \exp\left(-\mathrm{i}\frac{Et}{\hbar}\right)|\Psi_S(E,0)\rangle\,, \tag{19}$$

so $|\Psi_S(E,0)\rangle \equiv |\Psi_S(E)\rangle$ is a solution of the time-independent Schrödinger equation (7) (this justifies the use of the letter Ψ in Eq. (18)), and the Floquet ladder of quasienergies and the Wannier-Stark-ladder, $E_l = E_0 + 2\pi Fl$, coincide.

Relation (18) allows to use the asymptotes of the Floquet-Bloch-solution $|\Phi_S(E)\rangle$ (16) instead of the asymptotes of the $|\Psi_S(E)\rangle$ (7) in the S-matrix definition (9). As the time-evolution operator $U(\tau_B)$ commutes with the translation $x \to x + 2\pi$, we can choose the $|\Phi_S(E)\rangle$ to fulfill an additional Bloch-relation

$$|\Phi_S(E,x+2\pi)\rangle = \mathrm{e}^{\mathrm{i}2\pi\kappa}|\Phi_S(E,x)\rangle\,. \tag{20}$$

In other words, the $|\Phi_S(E)\rangle$ can be expressed using the plane waves

$$\langle x|n+\kappa\rangle = \frac{1}{\sqrt{2\pi}}\,\mathrm{e}^{\mathrm{i}(n+\kappa)x} \tag{21}$$

with $n \in \mathbb{Z}$ and $\kappa \in [-1/2, 1/2]$ as a basis set. On the other hand, $U(t) = \exp(-\mathrm{i}Ht/\hbar)$ can generally be expressed as a product of two operators [9],

$$U(t) = \mathrm{e}^{-\mathrm{i}Fxt/\hbar}\,\widetilde{U}(t)\,, \tag{22}$$

where

$$\widetilde{U}(t) = \widehat{\exp}\left(-\frac{\mathrm{i}}{\hbar}\int_0^t \widetilde{H}(t')\mathrm{d}t'\right) \tag{23}$$

with the time-dependent periodic Hamiltonian $\widetilde{H}(t) = (p - Ft)^2/2 + V(x)$ [9] (the hat over the exponential function denotes time ordering). In a plane wave basis, the operator $\exp(-\mathrm{i}Fxt/\hbar)$ acts as a momentum shift operator,

$$\mathrm{e}^{-\mathrm{i}Fxt/\hbar}|n+\kappa\rangle = |n+\kappa-Ft/\hbar\rangle\,. \tag{24}$$

Therefore, if we perform the integral (18) with $t = 0$, for $t' < \tau_B$ the integrand has a different Bloch index $\kappa' = \kappa - Ft'/\hbar$. However, when $t = \tau_B$, the Bloch indices coincide. Thus, at the points $k = n + \kappa$ the functions $\langle k|\Psi_S(E)\rangle$ and $\langle n+\kappa|\Phi_S(E)\rangle$ do coincide and we can insert the asymptotes of $|\Phi_S(E)\rangle$ in the S-matrix formula (9), i.e.

$$\mathbf{S}(E) = \lim_{n\to\infty} \frac{\langle -n+\kappa|\Phi_S\rangle}{\langle -n+\kappa|\Phi_0\rangle}\frac{\langle n+\kappa|\Phi_0\rangle}{\langle n+\kappa|\Phi_S\rangle}\,. \tag{25}$$

By construction $\mathbf{S}(E)$ in Eq. (25) is independent of κ, which provides a test for controlling the accuracy in numerical calculations.

2.3 Asymptotic properties of the Floquet-Bloch-solutions

Suppose, we choose $\kappa = 0$ and use the plane waves $\langle x|n\rangle$ with $n \in \mathbb{Z}$. For $t = \tau_B$ Eq. (22) gives

$$U(\tau_B) = \mathrm{e}^{-\mathrm{i}x}\,\widetilde{U}(\tau_B)\,. \tag{26}$$

In the plane wave basis we have $\langle m|\mathrm{e}^{-\mathrm{i}x}|n\rangle = \delta(m+1-n)$, thus $U(\tau_B)_{m,n} = \widetilde{U}(\tau_B)_{m+1,n}$. Then we can write Eq. (16) as a matrix eigenvalue equation. Introducing $C_n = \langle n|\Phi_S\rangle$ and $\lambda = \exp(-\mathrm{i}E\tau_B/\hbar)$, we have

$$\sum_n \widetilde{U}_{m+1,n}C_n = \lambda\, C_m\,. \tag{27}$$

For $n \to \pm\infty$, the kinetic term of the Hamiltonian dominates the potential and the matrix $\widetilde{U}$ tends to a diagonal one. Suppose, that this is sufficiently well fulfilled for $|n| > N$, i.e.

$$\widetilde{U}_{m,n} \approx u_m\delta_{m,n} \qquad \text{for } |m|,|n| > N \tag{28}$$

with

$$u_m = \exp\left(-\frac{\mathrm{i}}{2\hbar}\int_0^{\tau_B}(\hbar m - Ft')^2\,\mathrm{d}t'\right) \tag{29}$$

(note, that for the unscattered states $|\Phi_0\rangle$ this formula holds exactly for any m). Suppose we order C with indices increasing from bottom to top. Then we can decompose the vector C into three parts,

$$C = \begin{pmatrix} C^{(+)} \\ C^{(0)} \\ C^{(-)} \end{pmatrix}\,, \tag{30}$$

where $C^{(+)}$ contains the cofficients for $n > N$, $C^{(-)}$ contains the coefficients for $n < -N-1$ and $C^{(0)}$ contains all other coefficients for $-N-1 \le n \le N$. The coefficients of $C^{(+)}$ recursively depend on the coefficient C_N, via

$$C_{m+1} = (\lambda/u_{m+1})\,C_m \qquad \text{for } m \ge N\,. \tag{31}$$

Analogously, the coefficients of $C^{(-)}$ recursively depend on C_{-N-1}, via

$$C_m = (u_{m+1}/\lambda)\,C_{m+1} \qquad \text{for } m < -N-1\,. \tag{32}$$

Let us define the matrix W as the matrix $\widetilde{U}$, truncated to the size $N \times N$. Furthermore, let B be the matrix

$$B = \begin{pmatrix} \mathbf{0}^t & 0 \\ W & \mathbf{0} \end{pmatrix}\,. \tag{33}$$

Then the resulting equation for $C^{(0)}$ can be written as

$$(B - \lambda\mathbb{1})\,C^{(0)} = -u_{N+1}C_{N+1}e_N\,, \tag{34}$$

where e_N is a vector of the same length as C, with the first element equal to one and all others equal to zero. For a given λ, Eq. (34) links $C^{(+)}$, via C_{N+1} and Eq. (31), to $C^{(0)}$ and, via C_{-N-1} and Eq. (32), to $C^{(-)}$. Thus, Eq. (34) matches the asymptotes $C^{(+)}$ and $C^{(-)}$ and provides a tool to calculate the S-matrix elements [10]. Indeed, we will use Eq. (34) as the starting point for the calculation of the poles of the S-matrix.

2.4 Approximate calculation of the poles of the S-matrix

Let us recall the S-matrix definition for the Stark system,

$$\mathbf{S}(E) = \lim_{k\to\infty} \frac{\langle -k|\Psi_S\rangle}{\langle -k|\Psi_0\rangle}\frac{\langle k|\Psi_0\rangle}{\langle k|\Psi_S\rangle} = \lim_{n\to\infty} \frac{\langle -n+\kappa|\Phi_S\rangle}{\langle -n+\kappa|\Phi_0\rangle}\frac{\langle n+\kappa|\Phi_0\rangle}{\langle n+\kappa|\Phi_S\rangle}\,. \tag{35}$$

Resonances are defined as poles of the S-matrix. They correspond to scattering states with purely outgoing boundary conditions, i.e. with no incoming waves. Thus, to find the poles we have to look for zeros of the asymptotes of $\langle k|\Psi_S(E)\rangle/\langle k|\Psi_0(E)\rangle$. As we can see from Eq. (6), for complex energies $\mathcal{E} = E - \mathrm{i}\Gamma/2$ $\langle k|\Psi_0(\mathcal{E})\rangle$ exponentially goes to zero for $k \to \infty$, but $\langle k|\Psi_0(\mathcal{E})\rangle \neq 0$ for any finite k. Furthermore, as we can see from Eq. (8), the asymptotic part of $\langle k|\Psi_S(\mathcal{E})\rangle$ shows exactly the same asymptotic decay. Thus, if $C^{(+)} \neq 0$, we cannot have a pole.

On the other hand, if $\langle n+\kappa|\Phi_S(\mathcal{E})\rangle = 0$ (or $C_n = 0$) for one specific n with $n > |N|$, on the basis of the discussion of the last section, $C^{(+)} = 0$ follows recursively, i.e. $\langle n+\kappa|\Phi_S(\mathcal{E})\rangle = 0$ for $n > N$ (note, that this implies via eqs. (18), (22), (23) and (28), that $\langle k|\Psi_S(\mathcal{E})\rangle = 0$ for $k > N+\kappa$). Thus, in this case $\mathcal{E}$ is a pole of the S-matrix.

As the condition $C^{(+)} = 0$ implies a pole, let us take it as the starting point. Then, to calculate poles of the S-matrix we have to solve the matrix eigenvalue equation

$$(B - \lambda\mathbb{1})\, C^{(0)} = 0\,. \tag{36}$$

With increasing N, condition (28) is increasingly better fulfilled and the calculated eigenvalues converge to the poles of $\mathbf{S}(E)$.

2.5 Numerical example

As an example we calculate the resonances for the Hamiltonian

$$H = \frac{p^2}{2} + \cos(x) + Fx \tag{37}$$

with parameters $F = 0.07$ and $\hbar = 1.0$. Explicitly, we calculate the matrix $\widetilde{U}(\tau_\mathrm{B})$ (23), using $M = 2N+1$ plane wave basis states $\langle x|n\rangle$ via

$$\widetilde{U}(\tau_\mathrm{B}) = \prod_j \exp\left(-\frac{\mathrm{i}}{\hbar}\widetilde{H}(t_j)\Delta t\right) \tag{38}$$

where $t_j = (j-1/2)\Delta t$, $n \in \{1,2,\ldots,j_{max}\}$ and $\Delta t = \tau_B/j_{max}$. Then, by shifting the indices, we define the matrix B in (33) and calculate the eigenvalues λ of B. The resonance energies are given by $\mathcal{E} = \mathrm{i}F\ln\lambda$, where we used $\hbar/F = \tau_\mathrm{B}$.

The tables 1 and 2 show the three most stable resonances, i.e. those with the smallest imaginary parts, for different N (for $j_{max} = 100$). As a function of the matrix size, the numerical data converge surprisingly fast. Thus, we can perform the calculations using very small matrices. As a function of the second numerical parameter, the number of iterations, the results are almost converged. Indeed, an increase by a factor four yields a relative change in the results of the order 10^{-4}. Thus, the method provides a very effective tool for the calculation of Stark resonances.

N	$\mathrm{Re}(\mathcal{E}_0)$	$\mathrm{Re}(\mathcal{E}_1)$	$\mathrm{Re}(\mathcal{E}_2)$
4	1.22613427e-01	8.45333223e-02	-1.50463547e-01
6	1.22613060e-01	8.45367439e-02	-1.50413622e-01
8	1.22613060e-01	8.45367335e-02	-1.50410728e-01
10	1.22613060e-01	8.45367335e-02	-1.50410725e-01
15	1.22613060e-01	8.45367335e-02	-1.50410725e-01
15	1.22609152e-01	8.45328270e-02	-1.50414631e-01

Table 1. Real parts of the three most stable resonances of the system (37) for different N. The last line shows the results for $j_{max} = 400$.

N	$\mathrm{Im}(\mathcal{E}_0)$	$\mathrm{Im}(\mathcal{E}_1)$	$\mathrm{Im}(\mathcal{E}_2)$
4	-1.27758848e-08	-3.94827952e-04	-4.20424283e-02
6	-7.66948735e-10	-4.03118739e-04	-4.13651529e-02
8	-7.61555093e-10	-4.03129329e-04	-4.13664554e-02
10	-7.61560844e-10	-4.03129332e-04	-4.13664544e-02
15	-7.61555676e-10	-4.03129332e-04	-4.13664544e-02
15	-7.61557666e-10	-4.03129325e-04	-4.13664542e-02

Table 2. Imaginary parts of the same resonances for different N. The last line shows the results for $j_{max} = 400$.

3 Resonant tunneling

In the following sections we investigate the resonant tunneling of Wannier-Stark-resonances. To get a first glimpse on the subject, we calculate the resonances for the Hamiltonian (37) for different fields F with parameter $\hbar = 1.0$. In this case, the field-free Hamiltonian has two bands with energies well below the potential barrier. The mean energy of the third band is approximately one, i.e. close to the barrier. For this band, the energy $E(k)$ can be larger or smaller than the potential height. Thus, with the field switched on, we have two long lived states in each potential well (see also Tab. 2), which are related to the first two bands. The higher resonances are quite unstable.

Figure 1a) shows the calculated widths of the six most stable resonances as a function of the inverse field strength $1/F$. The two most stable resonances are clearly separated from the other resonances. The second excited resonance still can be distinguished from the other resonances, the lifetime of which is approximately the same. Looking at the lifetime of the most stable state, the most striking phenomenon is the existence of very sharp resonance-like structures, where within a small range of F the lifetime can decrease up to six orders of magnitude.

In Fig. 1b), we additionally depict the energies of the three most stable resonances as a function of the inverse field strength. As the Wannier-Stark-resonances are arranged in a ladder with spacing $\Delta E = 2\pi F$, we show only

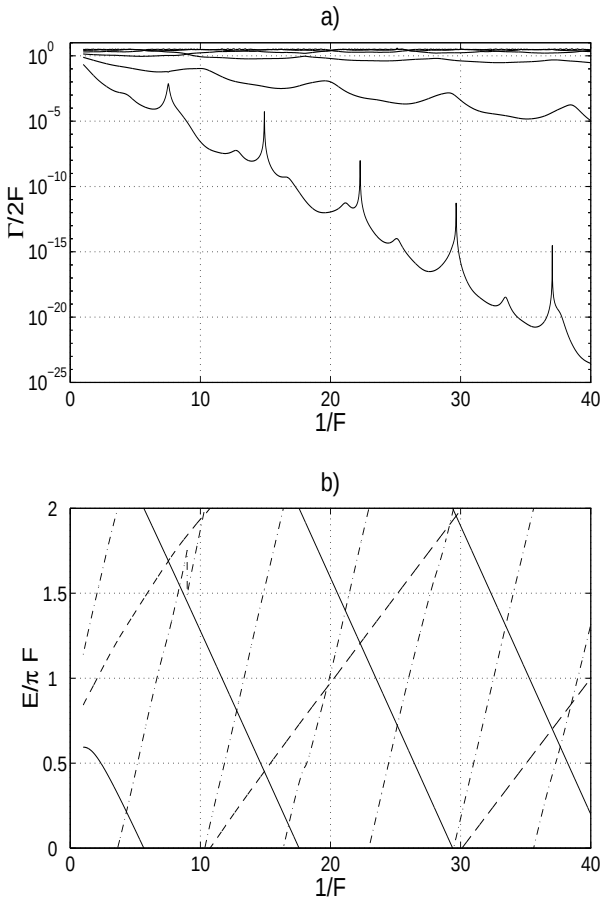

Fig. 1. a) Lifetime of the 6 most stable resonances as a function of $1/F$. b) Energies of the 3 most stable resonances as a function of $1/F$ (solid line: energy of the most stable resonance, dashed line: first excited resonance, dashed dotted line: second excited resonance). Parameters are $\hbar = 1.0$ and $N = 15$. The number of iterations j_{max} was adjusted $\propto 1/F$.

the energy interval $0 < E/F < 2\pi$, the first "Brillouin zone". Comparing with Fig. 1a), we find, that the decrease in lifetime coincides with crossings of the energies of the Wannier-Stark-resonances. All three possible crossings can be found in the lifetime figure 1a): Crossings of the two most stable resonances coincide with the sharpest peaks in the ground state width. The smaller peaks can be found at crossings of the ground state and the second excited state. Finally, crossings of the first and the second excited state fit to the peaks in the width of the first excited state.

The explanation of this effect is the following: Suppose we have a set of resonances which localize in one of the 2π-periodic minima of the potential $V(x) = \cos(x) + Fx$. Let $\Delta_{\alpha,\alpha'} = E_\alpha - E_{\alpha'}$ be the energy difference between two of these states. Now, due to the periodicity of the cosine, each resonance is a member of a Wannier-Stark-ladder of resonances, i.e. of a set of resonances with the same width, but with energies separated by $\Delta E = 2\pi F$. Thus, if two resonances of the same ladder are separated by l potential barriers, the splitting between both is $\Delta E = 2\pi F l$. Figure 2 shows an example: The two most stable resonances for one

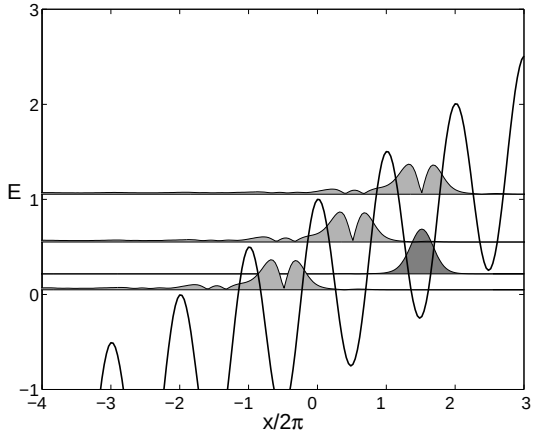

Fig. 2. Wannier-Stark-Resonances in different potential minima of $V(x) = \cos(x) + Fx$: The most stable resonance and some members of the first excited Wannier-Stark-ladder are shown. The parameters are $\hbar = 1.0$ and $F = 0.08$.

potential minimum are depicted, furthermore two other members of the Wannier-Stark-ladder of the first excited resonance. To decay, the ground state has to tunnel three barriers. Clearly, if there is a resonance with nearly the same energy in one of the adiacent minima, this will enhance the decay. The strongest effect will be given for degenerate energies, i.e. for $2\pi F l = \Delta_{\alpha,\alpha'}$, which can be achieved by properly adjusting F, because the splitting $\Delta_{\alpha,\alpha'}$ is nearly independent of the field strength.

For the case shown in Fig. 2, a degenerate case will occur, e.g. , for a slightly smaller value $F \approx 1/14.9$ (see Fig. 1). Then we have two resonances with the same energies, which are separated by two potential barriers. The less stable resonance enhances the decay of the more stable one (and, vice versa, the coupling between both resonances stabilizes the less stable one). Generally, the whole dependence of the width on the field in Fig. 1a) can be qualitatively explained by resonant tunneling: the strong peaks of the ground state width are due to resonant tunneling via one of the resonances in the first excited Wannier-Stark-ladder. The smaller peaks of the ground state width and the oscillations in the width of the first excited resonance are caused by the influence of the second excited Wannier-Stark-ladder. The influence of ladders of more unstable resonances seems to be neglibible. After we have a qualitative description of the resonant tunneling of the Wannier-Stark-states, the next sections will be devoted to a quantitative model description of the dependence of the widths on the field.

4 Two interacting Wannier-Stark-ladders

As resonant tunneling occurs, whenever the energy of one resonance coincides with the energy of one member of another Wannier-Stark-ladder, let us first look at the interaction of two single resonances and later extend the model to describe the interaction of whole Wannier-Stark-ladders.

The interaction of two resoances can be modeled by the 2×2-matrix

$$H = \begin{pmatrix} \mathcal{E}_0 & W \\ W & \mathcal{E}_1 \end{pmatrix} \tag{39}$$

with unperturbed resonance energies $\mathcal{E}_0 = E_0 - \mathrm{i}\Gamma_0/2$ and $\mathcal{E}_1 = E_1 - \mathrm{i}\Gamma_1/2$ and coupling W between both states. Introducing $\bar{E} = (E_0 + E_1)/2$, $\bar{\Gamma} = (\Gamma_0 + \Gamma_1)/2$, $\Delta E_{1,0} = E_1 - E_0$ and $\Delta\Gamma_{1,0} = \Gamma_1 - \Gamma_0$, the eigenvalues of the matrix H are

$$\mathcal{E}_\pm = \bar{E} - \mathrm{i}\bar{\Gamma}/2 \pm \sqrt{W^2 + \frac{1}{4}(\Delta E - \mathrm{i}\Delta\Gamma/2)^2}\,. \tag{40}$$

For $\Delta E = 0$ this yields

$$\mathcal{E}_\pm = \bar{E} - \mathrm{i}\bar{\Gamma}/2 \pm \sqrt{W^2 - (\Delta\Gamma/4)^2}\,. \tag{41}$$

Thus, varying ΔE, there are two possibilities: For $W > \Delta\Gamma/4$ we have the well-known curve-crossing scenario: there is a gap in the energies and the widths cross. For $\Delta E = 0$ both resonances have the same lifetime. On the other hand, for $W < \Delta\Gamma/4$, the energies cross, but the widths differ. For $\Delta E = 0$, the resonances have the same energies but different lifetimes. In Fig. 1 we see, that for the two most stable resonances the second case is realized exclusively. For the second excited resonance, the first case occurs once at $1/F \approx 9$, while for the more unstable resonances mainly crossings of the first kind appear.

In both cases, the less stable resonance is stabilized, while the more stable one is destabilized. However, the lifetime of the more stable resonance is much stronger influenced by the interaction. Indeed, the maximal stabilization, which the more unstable resonance can achieve, is a doubling of the lifetime, while, on the other hand, the lifetime of the more stable resonance can decrease by orders of magnitude.

Let us now adopt the description (39) for the case of two interacting Wannier-Stark-ladders, which is valid for large $\hbar$, where only one long-lived resonance exists. The degeneracy condition $\Delta E = 0$ has to be replaced by the more general condition, that the energies of the resonances coincide *modulo* the Wannier-Stark-splitting, i.e. by

$$\Delta E = 2\pi l F \tag{42}$$

with $l \in \mathbb{N}$. Let us rewrite the condition (42) as $\Delta E/F = 2\pi l$ and, using $\tau_\mathrm{B} = \hbar/F$ and $\Delta E = E_1 - E_0$, as

$$\mathrm{e}^{-\mathrm{i}E_1\tau_\mathrm{B}/\hbar} = \mathrm{e}^{-\mathrm{i}E_0\tau_\mathrm{B}/\hbar}, \tag{43}$$

which now looks like a condition for the quasiangles of two Floquet-Bloch-states. Thus, we will reformulate the model (39) in terms of Floquet-Bloch-solutions: The unperturbed matrix is then given by the diagonal matrix

$$U_0(F) = \begin{pmatrix} \mathrm{e}^{-\mathrm{i}(E_1 - \mathrm{i}\Gamma_1/2)/F} & 0 \\ 0 & \mathrm{e}^{-\mathrm{i}(E_0 - \mathrm{i}\Gamma_0/2)/F} \end{pmatrix}, \tag{44}$$

where we again used $\tau_\mathrm{B}/\hbar = 1/F$. We cannot include the coupling directly via the nondiagonal elements as in Eq. (39), since this would change the unitarity properties of the matrix. But, as the coupling results in mixing of the states, we can easily introduce it by applying a rotation to $U_0(F)$. The final matrix $U(F)$ is then given by [11]

$$U(F) = U_0(F)\,\mathrm{e}^{-\mathrm{i}W/F}\,, \tag{45}$$

where the interaction matrix shall be given by

$$W = \begin{pmatrix} 0 & w \\ w & 0 \end{pmatrix}. \tag{46}$$

The eigenvalues of $U(F)$, Eq. (45), can be calculated analytically. Introducing

$$\lambda_{0,1} = \exp\left(-\mathrm{i}\frac{\mathcal{E}_{0,1}}{F}\right), \quad \mathcal{E}_{0,1} = E_{0,1} - \mathrm{i}\frac{\Gamma_{0,1}}{2}, \tag{47}$$

we get the eigenvalues

$$\begin{aligned} \widetilde{\lambda}_{0,1} &= \cos(w/F)\,\frac{\lambda_0 + \lambda_1}{2} \\ &\pm \sqrt{\cos^2(w/F)\left(\frac{\lambda_0 + \lambda_1}{2}\right)^2 - \lambda_0\lambda_1}\,, \end{aligned} \tag{48}$$

which for $w/F << 1$ yields for the ground state

$$\widetilde{\lambda}_0 = \lambda_0\left(1 - \frac{1}{2}\left(\frac{w}{F}\right)^2 \frac{\lambda_0 + \lambda_1}{\lambda_0 - \lambda_1}\right). \tag{49}$$

Assuming again $w/F << 1$, we get the following correction for Γ_0

$$\frac{\Delta\Gamma_0}{F} = \left(\frac{w}{F}\right)^2 \mathrm{Re}\left[\frac{\lambda_0 + \lambda_1}{\lambda_0 - \lambda_1}\right]. \tag{50}$$

To check the validity of formula (50) for the description of the overall behaviour of the resonance widths (as a function of the inverse field strength) with this model, we have to make assumptions on the dependence of the parameters on the field F. We start with the energies. The additional field causes an energy shift of the potential minimum by πF and a deformation of the field-free cosine potential. While the minimum shift affects all energies in the same way, the deformation has a stronger impact on the higher lying states. Therefore, let us take the deformation into account by assuming a linear dependence on the field, i.e. $E_\alpha(F) = E_\alpha + D_\alpha F$, with constants E_α, D_α(note, that in Eq. (50) we only need the difference between both energies). Second, by hand we set $\Gamma_0 = 0$ for the ground state width. Finally, for Γ_1 and the coupling w we assume a smooth dependence on the field as predicted by Zener theory [12], i.e.

$$\begin{aligned} \Gamma_1/2 &= a\,F\exp(-c/F) \\ w &= b\,F\exp(-d/F) \end{aligned} \tag{51}$$

with constants a, b, c, d.

To test the model we calculated the resonances widths for the case $\hbar = 1.671$ (this value corresponds to the settings in the experiment [7]). In this case, only the ground

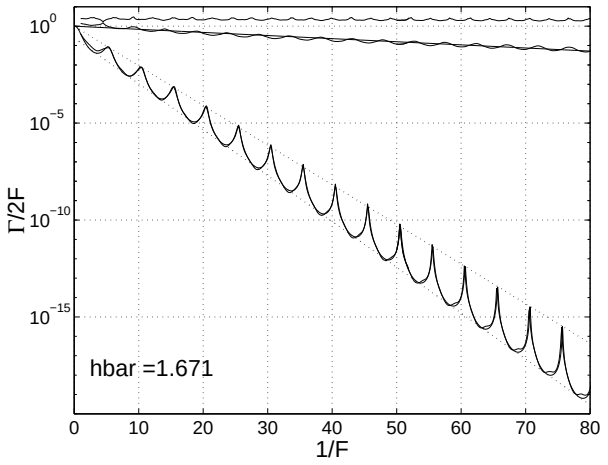

Fig. 3. Widths of the three most stable resonances as a function of the inverse field strength F for $\hbar = 1.671$ (solid lines). A fit using the two state model is added (solid lines, see text). The dotted lines are the model predictions for the amplitude of the lifetime modulation.

band of the field-free Hamiltonian can support long-lived states. The average energy of the first excited band of the field-free Hamiltonian is $E_1 = 0.9846$, and already the first excited resonance is expected to be short lived. Therefore the two-state description should be applicable.

The six model parameters were determined in the following way: First, the parameters a and c were chosen such that the curve $\Gamma_1(F)$ fits the mean behaviour of the calculated width of the first excited resonance, i.e. $a = 1.0$ and $c = 0.037$ (see the straight solid line in the lifetime of the first excited state in figure 3). Second, we took E_α as the averaged energy of the α-th band of the field-free Hamiltonian, which yields $E_1 - E_0 = 1.2501$. While this parameter determines the frequency of the oscillation of the width, the parameter $D = D_1 - D_0$ yields an additional phase shift between λ_1 and λ_0 and therefore shifts the maxima of the widths. It was chosen as $D = -0.4$. Finally, the interaction parameters $b = 1.0$ and $d = 0.254$ were chosen to yield the mean behaviour of the ground state width.

As demonstrated in Fig. 3, the calculated and the fitted curve overlap almost perfectly. Thus the numerical data are very well approximated by the model (up to some additional small oscillations which reflect the influence of higher excited Wannier-Stark-ladders). Assuming $\Gamma_1/F << 1$, one can immediately deduce from Eq. (50) the maximum and the minimum width of the ground state as

$$\frac{\Gamma_{max,min}}{F} = \left(\frac{w}{F}\right)^2 \left(\frac{\Gamma_1}{4F}\right)^{\mp 1} \tag{52}$$

(note, that the amplitude of the oscillation increases proportional to Γ_1^{-2}, i.e. exponentially). The resulting curves (dotted lines in Fig. 3) correctly describe the calculated data. Summarizing, the model (45) yields an appropriate description of the ground state width behaviour for the case of large $\hbar$, where we only have one long-lived resonance.

5 Few ladder case

For smaller values of $\hbar$, the field-free Hamiltonian has more than one band with mean energy smaller than the potential barrier, and therefore, the full Hamiltonian has more than one, say M, long-lived states. Then, the model description has to take into account the interaction of $M+1$ Wannier-Stark-ladders. In the following, a hierarchical, Born-Oppenheimer-like approach will be developed, which is shown to correctly model the behaviour of the widths.

5.1 Model extension for three interacting ladders

The most simple extension is given for the case of two long lived resonances as, e.g., for $\hbar = 1.0$ (see Fig. 1a)). As already discussed above, we then have to additionally take into account the interaction with the second excited resonance ladder. The setup is as follows: Let us assume we have three unperturbed states with energies $\mathcal{E}_\alpha = E_\alpha - \mathrm{i}\Gamma_\alpha/2$. We first construct the unperturbed Floquet matrix $U_0(F)$,

$$U_0(F) = \begin{pmatrix} \lambda_2 & 0 & 0 \\ 0 & \lambda_1 & 0 \\ 0 & 0 & \lambda_0 \end{pmatrix} , \tag{53}$$

with λ_α defined as in Eq. (47). Let us, as before, add the interaction by multiplication with a unitary matrix $\in SU(3)$. Assuming that the interaction of the first and the second excited ladder is much "faster" than the interaction with the ground ladder, we introduce the coupling by two successive rotations,

$$U(F) = U_0(F)\, \mathrm{e}^{-\mathrm{i}W_{12}/F}\, \mathrm{e}^{-\mathrm{i}W_{01}/F} , \tag{54}$$

where W_{12} describes the coupling between λ_2 and λ_1,

$$W_{12} = \begin{pmatrix} 0 & w_1 & 0 \\ w_1 & 0 & 0 \\ 0 & 0 & 0 \end{pmatrix} , \tag{55}$$

and W_{01} describes the coupling between λ_0 and λ_1,

$$W_{01} = \begin{pmatrix} 0 & 0 & 0 \\ 0 & 0 & w_0 \\ 0 & w_0 & 0 \end{pmatrix} . \tag{56}$$

As the matrix exponents of W_{01} and W_{12} are known analytically, we can further evaluate Eq. (54). The eigenvalues $\widetilde{\lambda}$ fulfill

$$\begin{aligned} \lambda_2\lambda_1\lambda_0 - \widetilde{\lambda}(\lambda_2\lambda_1 c_0 + \lambda_2\lambda_0 c_1 c_0 + \lambda_1\lambda_0 c_1) \\ +\widetilde{\lambda}^2(\lambda_2 c_1 + \lambda_1 c_1 c_0 + \lambda_0 c_0) - \widetilde{\lambda}^3 = 0 \end{aligned} \tag{57}$$

where we introduced $c_\alpha = \cos(\epsilon_\alpha)$ with $\epsilon_\alpha = w_\alpha/F$. To calculate the additional width of the ground state, we insert the ansatz $\widetilde{\lambda}_0 = \lambda_0(1+\delta_0)$ into this equation and take into account terms up to the first order in δ_0. Furthermore, we approximate $c_\alpha \approx 1 - \epsilon_\alpha^2/2$, which yields

$$\begin{aligned} -\frac{\epsilon_0^2}{2} & \left[(\lambda_0+\lambda_1)(\lambda_0-\lambda_2) - \frac{\epsilon_1^2}{2}\lambda_0(\lambda_1-\lambda_2)\right] \qquad (58)\\ = \delta_0 & \left[(\lambda_0-\lambda_1)(\lambda_0-\lambda_2) + \frac{\epsilon_1^2}{2}\lambda_0(\lambda_1+\lambda_2)\right.\\ & \left. + \frac{\epsilon_0^2}{2}(\lambda_0+\lambda_1)(2\lambda_0-\lambda_2) - \frac{\epsilon_0^2\epsilon_1^2}{4}\lambda_0(2\lambda_1-\lambda_2)\right] \end{aligned}$$

As we have $\delta_0 \sim \epsilon_0^2$, the error caused by neglecting higher orders in δ_0 is proportional to $\delta_0\epsilon_0^2$. Therefore, the third line in equation (58) corresponds to a correction of order δ_0^2 and can be neglected with the result

$$\delta_0 = -\frac{\epsilon_0^2}{2}\,\frac{(\lambda_0+\lambda_1)(\lambda_0-\lambda_2) - \frac{\epsilon_1^2}{2}\lambda_0(\lambda_1-\lambda_2)}{(\lambda_0-\lambda_1)(\lambda_0-\lambda_2) + \frac{\epsilon_1^2}{2}\lambda_0(\lambda_1+\lambda_2)}. \qquad (59)$$

Because of $\widetilde{\lambda}_0 = \exp(-\mathrm{i}\mathcal{E}_0/F)$, the ground state width is given by the negative real part of the logarithm of $\widetilde{\lambda}_0$. Approximating $\ln(1+\delta_0) \approx \delta_0$, we directly get the first order correction to the ground state width as

$$\frac{\Delta\Gamma_0}{F} = \epsilon_0^2\,\mathrm{Re}\left[\frac{(\lambda_0+\lambda_1)(\lambda_0-\lambda_2) - \frac{1}{2}\epsilon_1^2\lambda_0(\lambda_1-\lambda_2)}{(\lambda_0-\lambda_1)(\lambda_0-\lambda_2) - \frac{1}{2}\epsilon_1^2\lambda_0(\lambda_1+\lambda_2)}\right]. \qquad (60)$$

To compare the model with numerical calculations, we proceed as in the previous section: Let us assume a linear field dependence of the energies, $E_\alpha(F) = E_\alpha + D_\alpha F$, and let us set $\Gamma_1 = \Gamma_0 = 0$. Furthermore, let us assume the Zener type formulas

$$\begin{aligned} \Gamma_2/2 &= a\ F\exp(-c/F)\\ w_0 &= b_0 F\exp(-d_0/F)\\ w_1 &= b_1 F\exp(-d_1/F) \end{aligned} \qquad (61)$$

Figure 4 shows again the widths of the six most stable states from Fig. 1a), but now compared with the predictions of the three-state model (54). The model parameters were determined the following way: The energies E_α were calculated independently from the average band energies of the first three bands of the field-free Hamiltonian, i.e. $E_0 = -0.5337$, $E_1 = 0.3154$ and $E_2 = 0.9806$. Then, first the width of the second excited ladder was chosen to yield the average behaviour of the third calculated resonance, i.e. $a = 1.2$ and $c = 0.036$. Next, we adjusted the parameters for the first excited ladder following the two-state formula (50). Explicitly, we took $b_1 = 1.1$, $d_1 = 0.13$ and $D_2 - D_1 = -0.35$. Finally, following Eq. (60), the parameters for the most stable ladder were determined as $b_0 = 0.9$, $d_0 = 0.50$ and $D_1 - D_0 = -0.05$.

Over many orders of magnitude, the model data fit almost perfectly to the calculated widths. The main deviations in $\Gamma_1(F)$ appear at very small F, where the first

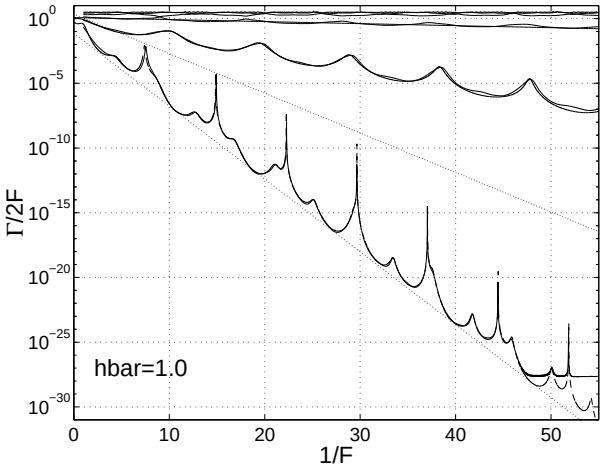

Fig. 4. Widths of the six most stable resonances as a function of the inverse field F for $\hbar = 1.0$ (straight lines) compared with the fit data (dashed lines).

effects due to the interaction with the third excited Wannier-Stark-ladder show up. The ground state width is accurately described over the whole range (the deviation at the end is due to finite numerical accuracy).

Further evaluation of Eq. (60) yields additional predictions about the oscillation of the widths. E.g., the oscillation is bounded by the curves

$$\frac{\Gamma_{\max,\min}}{F} = \epsilon_0^2\left(\frac{\epsilon_1^2\Gamma_2}{16F}\right)^{\mp 1} = \epsilon_0^2\left(\frac{\Gamma_{1,\max}}{4F}\right)^{\mp 1} \qquad (62)$$

which are additionally depicted in the figure (dotted lines). The minima fit pretty well. Concerning the maximal values, a closer inspection of Eq. (60) yields, that they appear, when $\lambda_0 = \lambda_1 = -\lambda_2/|\lambda_2|$ is fulfilled, i.e. when the ground and the first ladder cross, while the first and the second ladder "anticross". This is nearly the case for the first three maxima, which Eq. (62) correctly describes. The deviation at the last two peaks, where the twofold resonance condition is fulfilled again, is due to the data resolution (finite step in $1/F$).

Concluding, the extended model correctly predicts the oscillation of the width for the given case of two long-lived resonances. The main model assumption is, that the most stable Wannier-Stark-ladder is directly coupled only to the next ladder and that the coupling to all other ladders is indirect. Therefore, starting from the first "short-lived" ladder, we can treat the more stable ladders successively: When we have a set of interacting Wannier-Stark-ladders and additionally take into account the interaction with a more stable one, the lifetime of the previous set is almost unchanged by this procedure. Thus, for every step, we only have to adjust the parameters for the new ladder. In the next subsection, we generally describe this hierarchical mechanism and apply it to a five state case.

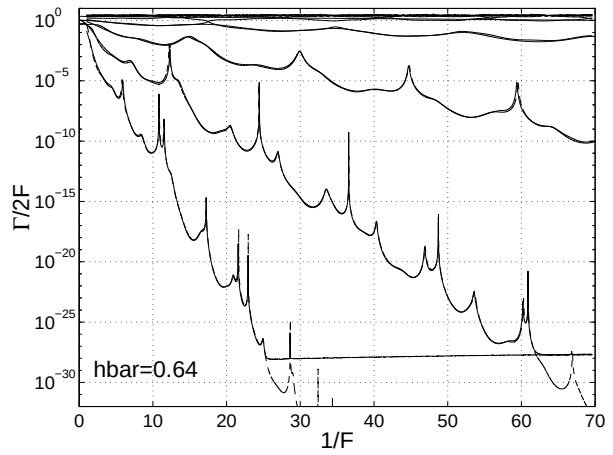

Fig. 5. Widths of the ten most stable resonances as a function of the inverse field F for $\hbar = 0.64$ (straight lines) compared with the fit data (dashed lines) from the model (64) for $M = 4$.

5.2 Hierarchical description: five ladders

Following the ideas of the previous section, we extend the model to the case, where the Hamiltonian supports M long-lived resonances, while all other resonances are short-lived with approximately the same lifetime. Thus, taking into account the long-lived states and the first short-lived one, we use a $M+1$-state description. The prescription is as follows: start with the unperturbed Floquet matrix

$$U_0(F) = \begin{pmatrix} \lambda_{M+1} & 0 & \dots & & & \\ 0 & \lambda_M & \dots & & & \\ \vdots & \vdots & \ddots & & & \\ & & & \lambda_2 & 0 & 0 \\ & & & 0 & \lambda_1 & 0 \\ & & & 0 & 0 & \lambda_0 \end{pmatrix}, \tag{63}$$

where λ_α is given as in Eq. (47), and successively add the interaction by a series of multiplications, i.e.

$$U(F) = U_0(F)\, \mathrm{e}^{-\mathrm{i}W_{M,M+1}/F} \dots \mathrm{e}^{-\mathrm{i}W_{12}/F}\, \mathrm{e}^{-\mathrm{i}W_{01}/F}, \tag{64}$$

where

$$(W_{\alpha,\alpha+1})_{n,n'} = (\delta_{\alpha,n}\, \delta_{\alpha+1,n'} + \delta_{\alpha,n'}\, \delta_{\alpha+1,n})\, w_\alpha\,. \tag{65}$$

For the w_α and Γ_{M+1}, assume a Zener-type formula as in Eq. (61), for the energies assume $E_\alpha(F) = E_\alpha + D_\alpha F$. The E_α can be calculated independently as the average energies of the α-th Bloch band of the field-free Hamiltonian. Furthermore, by hand set $\Gamma_M = \dots = \Gamma_0 = 0$ and $D_{M+1} = 0$. Then, start with the $M+1$-th ladder and adjust the parameters for Γ_{M+1}. Successively, take into account the more stable ladders. For $\alpha = M, M-1, \dots, 0$, first adjust the mean behaviour of the α-th width by the parameters b_α and d_α. Then, shift the maxima to the correct position by adjusting the D_α.

One can use Eq. (64) as a basis for a numerical evaluation. On the other hand, one can take it as a starting point for a perturbation theoretical analysis of the additional width, the most stable state gets due to the interaction with the other states. The second approach follows directly the procedure described in the previous section.

We insert the ansatz $\widetilde{\lambda}_0 = \lambda_0(1+\delta_0)$ into the characteristic polynomial and take into account the first order in δ_0. Then, we approximate $c_\alpha \approx 1 - \epsilon_\alpha^2$. As before, we have $\delta_0 \sim \epsilon_0^2$, therefore we neglect all factors with $\delta_0\epsilon_0^2$. The calculation yields no additional information, therefore we just display the results. Let us present the additional width the ground state gets in the form

$$\frac{\Delta\Gamma_0}{F} = \epsilon_0^2\, \frac{f_M(\lambda,\epsilon)}{g_M(\lambda,\epsilon)}\,. \tag{66}$$

For the case $M = 3$, the functions $f_3(\lambda,\epsilon)$ and $g_3(\lambda,\epsilon)$ are

$$\begin{aligned} f_3(\lambda,\epsilon) &= (\lambda_0+\lambda_1)(\lambda_0-\lambda_2)(\lambda_0-\lambda_3) \\ &\quad - \frac{\epsilon_1^2}{2}\lambda_0(\lambda_1-\lambda_2)(\lambda_0-\lambda_3) \\ &\quad + \frac{\epsilon_2^2}{2}\lambda_0(\lambda_0+\lambda_1)(\lambda_2+\lambda_3) \\ &\quad - \frac{\epsilon_1^2\epsilon_2^2}{4}\lambda_0(\lambda_0\lambda_2+\lambda_1\lambda_3)\,, \\ g_3(\lambda,\epsilon) &= (\lambda_0-\lambda_1)(\lambda_0-\lambda_2)(\lambda_0-\lambda_3) \\ &\quad + \frac{\epsilon_1^2}{2}\lambda_0(\lambda_1+\lambda_2)(\lambda_0-\lambda_3) \\ &\quad + \frac{\epsilon_2^2}{2}\lambda_0(\lambda_0-\lambda_1)(\lambda_2+\lambda_3) \\ &\quad - \frac{\epsilon_1^2\epsilon_2^2}{4}\lambda_0(\lambda_0\lambda_2-\lambda_1\lambda_3)\,. \end{aligned} \tag{67}$$

Similarly, in the case $M = 4$ we get for the functions $f_4(\lambda,\epsilon)$ and $g_4(\lambda,\epsilon)$

$$\begin{aligned} f_4(\lambda,\epsilon) &= (\lambda_0-\lambda_4) f_3(\lambda,\epsilon) \\ &\quad + \frac{\epsilon_3^2}{2}\lambda_0(\lambda_0+\lambda_1)(\lambda_0-\lambda_2)(\lambda_3+\lambda_4) \\ &\quad - \frac{\epsilon_1^2\epsilon_3^2}{4}\lambda_0^2(\lambda_1-\lambda_2)(\lambda_3+\lambda_4) \\ &\quad - \frac{\epsilon_2^2\epsilon_3^2}{4}\lambda_0(\lambda_0+\lambda_1)(\lambda_0\lambda_3-\lambda_2\lambda_4) \\ &\quad + \frac{\epsilon_1^2\epsilon_2^2\epsilon_3^2}{8}\lambda_0^2(\lambda_1\lambda_3-\lambda_2\lambda_4)\,, \\ g_4(\lambda,\epsilon) &= (\lambda_0-\lambda_4) g_3(\lambda,\epsilon) \\ &\quad + \frac{\epsilon_3^2}{2}\lambda_0(\lambda_0-\lambda_1)(\lambda_0-\lambda_2)(\lambda_3+\lambda_4) \\ &\quad + \frac{\epsilon_1^2\epsilon_3^2}{4}\lambda_0^2(\lambda_1+\lambda_2)(\lambda_3+\lambda_4) \\ &\quad - \frac{\epsilon_2^2\epsilon_3^2}{4}\lambda_0(\lambda_0-\lambda_1)(\lambda_0\lambda_3-\lambda_2\lambda_4) \\ &\quad - \frac{\epsilon_1^2\epsilon_2^2\epsilon_3^2}{8}\lambda_0^2(\lambda_1\lambda_3+\lambda_2\lambda_4)\,. \end{aligned} \tag{68}$$

Note that each term in the functions $f_M(\lambda,\epsilon)$ has its analogue in the functions $g_M(\lambda,\epsilon)$, and, basically, both functions differ only in the signs.

Figure 5 shows a comparison with the numerical data for $\hbar = 0.64$, where we have approximately four long-lived states. The model parameters were determined as described above, they are

$$\begin{aligned} E_4 &= +1.1945,\, D_4 = 0.00,\;\; a = 2.2,\;\;\; \alpha = 0.011 \\ E_3 &= +0.8327,\, D_3 = 0.10,\, b_3 = 1.30,\, d_3 = 0.026 \\ E_2 &= +0.4063,\, D_2 = 0.35,\, b_2 = 1.00,\, d_2 = 0.129 \\ E_1 &= -0.1099,\, D_1 = 0.38,\, b_1 = 0.92,\, d_1 = 0.361 \\ E_0 &= -0.6934,\, D_0 = 0.44,\, b_0 = 0.90,\, d_0 = 0.712. \end{aligned} \tag{69}$$

The fit perfectly models the numerical data (as before, the deviation in the end is due to finite numerical accuracy). Indeed, the width of the third excited state follows the two-state prediction, while the width of the first and the second excited state is similar to the ground state width in Fig. 4. In the ground ladder the structure is more complicated and visually one cannot clearly assign the direct correspondence of individual peaks and crossings.

6 Conclusions

In 1982, Avron conjectured that due to resonant tunneling the lifetime of the Wannier-Stark-states should be a complicated functions of the inverse field strength [13]. The conjecture was checked by Grecchi et al. for a Kronig-Penney model with a steplike field [14]. Using a new approach for the calculation of resonances in Stark systems, we were able to calculate the lifetime without any approximations and to check the conjecture this way. For large scaled $\hbar$, where only one or two long-lived resonances exist, the lifetime shows strong oscillations. Nevertheless, the dependence is well structured. For small $\hbar$, e.g. for $\hbar < 0.64$, where more than four ladders interact, the structure is indeed pretty complicated. Thus, it depends mainly on the value of the scaled Planck constant which case is realized. The experiments [4–6] correspond to values $\hbar \geq 1.5$, thus to the one-ladder case. Nevertheless, the four-ladder case $\hbar = 0.64$ seems not to be out of reach experimentally.

The few state model allows to describe the dependence of the widths by few parameters which in this paper were determined by a fit. Generally, it is desirable to calculate the parameters independently, which then yields a complete description of the resonant tunneling. This work is still in progress.

This research has been supported by the Deutsche Forschungsgemeinschaft (SPP 'Zeitabhängige Phänomene und Methoden in Quantensystemen der Physik und Chemie').

References

1. J. B. Krieger and G. J. Iafrate, Phys. Rev. B **33** (1986) 5494
2. G. Nenciu, Rev. Mod. Phys. **63** (1991) 91
3. F. Rossi, Semicond. Sci. Technol. **13** (1998) 147
4. S. R. Wilkinson, C. F. Bharucha, K. W. Madison, Qian Niu, and M. G. Raizen, Phys. Rev. Lett. **76** (1996) 4512
5. M. B. Dahan, E. Peik, J. Reichel, Y.Castin, and C. Salomon, Phys. Rev. Lett. **76** (1996) 4508
6. M. G. Raizen, C. Salomon, and Qian Niu, Physics Today July (1997) 30
7. C. F. Bharucha, K. W. Madison, P. R. Morrow, S. R. Wikinson, B. Sundaram, and M. G. Raizen, Phys. Rev. A **55** (1997) R857
8. J. Zak, J.Phys. Cond. Mat. **8** (1996) 8295
9. M. Glück, A. R. Kolovsky, H. J. Korsch, and N. Moiseyev, Eur. Phys. J. D **4** (1998) 239
10. M. Glück, A. R. Kolovsky, and H. J. Korsch, Phys. Rev. Lett. **82** (1999) 1534
11. M. Glück, A. R. Kolovsky, and H. J. Korsch, Phys. Rev. Lett. **83** (1999) 891
12. C. Zener, Proc. Roy. Soc. Lond. A **145** (1934) 523
13. J. E. Avron, Ann. Phys. (N.Y.) **143** (1982) 33
14. F. Bentosela, V. Grecchi, and F. Zironi, Phys. Rev. Lett. **50** (1982) 84